

Solution of Radiation and Scattering Electromagnetic Problems in Cartesian, Spherical and Cylindrical Coordinates by Green's Function Method

Sergey Knyazev, Boris Panchenko, and Sergey Shabunin

Abstract—The method of Green's functions for layered magneto-dielectric structures with arbitrary extraneous electric and magnetic currents is described. Application peculiarities of the method for Cartesian, cylindrical and spherical coordinate system are under consideration. The equivalent circuit approach is applied for layered structures description. Transmitting matrices are used for wave propagation modelling in each layer and through boundaries between layers. It is shown that the boundary transmitting matrix for flat and spherical structures is equal to the unit matrix. Different kinds of loads are used for region boundaries modelling. Suggested method with transmitting matrices allows one to develop universal algorithms with common modules for wave propagation, antennas radiation and scattering problems associated with flat, cylindrical and spherical structures of any number of layers, arbitrary permittivity and permeability. As an example, the problem of minimizing the reflection from a perfectly conducting surface with a two-layer cover using the Green's functions method is considered.

Keywords—Green's function, radiation, scattering, layered structures, reflection, electromagnetic waves.

I. INTRODUCTION

COMPUTER simulation software such as the Ansys HFSS, FEKO, CST Microwave Studio is widely used in microwaves and radio engineering electromagnetic design. Modern computers can carry out complicated electrodynamic radiation, propagation and scattering problems [1]–[4]. Algorithms of modern software used for electromagnetic modeling are based on splitting the analyzed objects into elementary elements and applying numerical methods such as the finite element method and finite difference method. However, use of the numerical algorithms embedded in most software products leads to significant processing time and resource costs. Calculations are greatly complicated in the presence of layered media with different electro-physical

parameters. As an example of such kind of problems the Luneburg lens radiation calculation and the synthesis of non-reflecting coatings can be mentioned [5], [6].

Application of algorithms based on analytical approaches allows one to speed up electromagnetic calculations essentially. This is particularly true if optimization procedure of geometrical and electrical properties of microwave devices and electro-physical properties of applied materials is used. The limitation of the analytical methods is the requirement of consistency of analyzed objects shape with coordinate systems. In spite of this fact the mentioned approach may be successfully used for a lot of radiation, excitation, propagation and scattering problems solving as the first step before electromagnetic simulation. For example, it is fruitful for nonreflecting covers design and optimization. Before optimizing the complex shape cover, the flat structure can be optimized. The advantage of analytical methods is the understanding of the observed physical processes.

In this paper, we consider the application of the Green's function method for solving electromagnetic excitation, diffraction and radiation problems. Our way of solution allows us to solve electromagnetic problems in different coordinate systems using the same approach and similar algorithms. To describe the observed processes, the same models are used in electromagnetic modeling. The proposed approach allows one to create fast algorithms for electrodynamic problems solving in particular with areas containing layered magneto-dielectrics. The equivalent electrical circuit approach is applied for layered structure modelling. Transmitting matrixes are used for wave propagation through layers and boundaries between layers' calculation. Different kinds of loads are used for region boundaries modelling. Green's functions for Cartesian, cylindrical, and spherical regions are shown and compared. Suggested method allows one to produce universal algorithms with common modules for electromagnetic wave propagation, antennas radiation and scattering problems associated with flat, cylindrical and spherical structures of any number of layers with arbitrary permittivity and permeability. Materials with negative refraction index (metamaterials) may be considered as well.

This work was supported by the grant of the Ministry of education and science of the Russian Federation (project № 8.2538.2017/4.6).

Sergey Knyazev is with the Ural Federal University, Ekaterinburg, 620002, Russia (e-mail: s.t.knyazev@urfu.ru).

Boris Panchenko is with the Ural Federal University, Ekaterinburg, 620002, Russia (e-mail: val.perminova@yandex.ru).

Sergey Shabunin is with the Ural Federal University, Ekaterinburg, 620002, Russia (corresponding author; e-mail: shab@ieec.org).

II. GREEN'S FUNCTIONS FOR CARTESIAN, CYLINDRICAL AND SPHERICAL LAYERED STRUCTURES

Almost all radiation and scattering problems can be solved using elementary radiation sources, such as an electric dipole, a magnetic dipole, and a Huygens element [3]. The latter is a combination of electric and magnetic dipoles. Thus, only two types of extraneous sources can be considered as an exciter of electromagnetic fields. Radiated and scattered electromagnetic fields from any antenna or irradiated object can be obtained by integrating electric and magnetic currents distributed on the antenna or object surface.

An electromagnetic field in any point of view defined by vector \mathbf{r} generated by extraneous electric $\mathbf{J}(\mathbf{r}')$ and/or magnetic $\mathbf{M}(\mathbf{r}')$ source current density located in the point of the source region V' defined by vector \mathbf{r}' is calculated as follows

$$\mathbf{E}(\mathbf{r}) = \int_{V'} \left[\bar{\bar{\Gamma}}_{11}(\mathbf{r}, \mathbf{r}') \mathbf{J}(\mathbf{r}') + \bar{\bar{\Gamma}}_{12}(\mathbf{r}, \mathbf{r}') \mathbf{M}(\mathbf{r}') \right] dv', \quad (1)$$

$$\mathbf{H}(\mathbf{r}) = \int_{V'} \left[\bar{\bar{\Gamma}}_{21}(\mathbf{r}, \mathbf{r}') \mathbf{J}(\mathbf{r}') + \bar{\bar{\Gamma}}_{22}(\mathbf{r}, \mathbf{r}') \mathbf{M}(\mathbf{r}') \right] dv', \quad (2)$$

where $\bar{\bar{\Gamma}}_{11}(\mathbf{r}, \mathbf{r}')$, $\bar{\bar{\Gamma}}_{22}(\mathbf{r}, \mathbf{r}')$, $\bar{\bar{\Gamma}}_{12}(\mathbf{r}, \mathbf{r}')$, $\bar{\bar{\Gamma}}_{21}(\mathbf{r}, \mathbf{r}')$ are the electric, magnetic and "transfer" Green's function, respectively [7]. Taking into account the vector nature of the electromagnetic field each tensor in (1), (2) is a matrix of the 3rd order. The type of the functions significantly depends on the used coordinate system. The most applicable are Cartesian, cylindrical and spherical coordinate systems. The solution will be much easier if the boundaries between layers are perpendicular to only one of the coordinates (Fig.1). For the Cartesian system all axes are equal, but as such we use the axis z . For cylindrical and spherical regions, the boundaries are perpendicular to the radial coordinate. The environment remains homogeneous along the other two coordinates. The Fourier type decomposition is used for these cross sections.

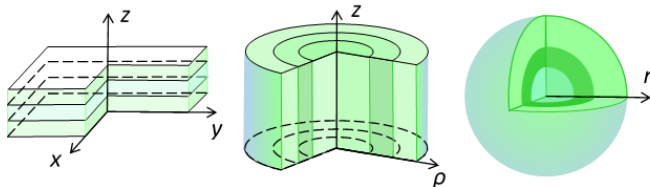


Fig. 1 The layered structure in Cartesian, cylindrical and spherical coordinate systems

The part of the Green's function which describes the inhomogeneous medium along the chosen coordinate axis is denoted as characteristic part. The characteristic part is found from the differential equation solution taking into account the boundary conditions. The problem is simplified by using the representation of electromagnetic field as the combination of electric and magnetic waves. In this case, two modal transmission lines describe an inhomogeneous medium (Fig.2). Electric and magnetic spectral field components are equated to the modal voltages and currents in the equivalent E - and H -

lines [7]. This is a consequence of the fact that the Maxwell equations in the decomposition of E and H waves become similar to the telegrapher's equations with currents and voltages in the long line model.

At the stage of the formulas derivation, various boundary conditions are taken into account. There are several types of region boundaries as follows: unlimited space, a perfect or real conductors placed in sections $\tau = \tau_1$ and $\tau = \tau_N$, as well as a magneto-dielectric medium for $\tau = 0$ in cylindrical and spherical coordinate system, if there is no conductive boundary in the direction of decreasing the τ coordinate. The generalized coordinate τ corresponds to the coordinate z , ρ or r in Cartesian, cylindrical, and spherical coordinate system, respectively.

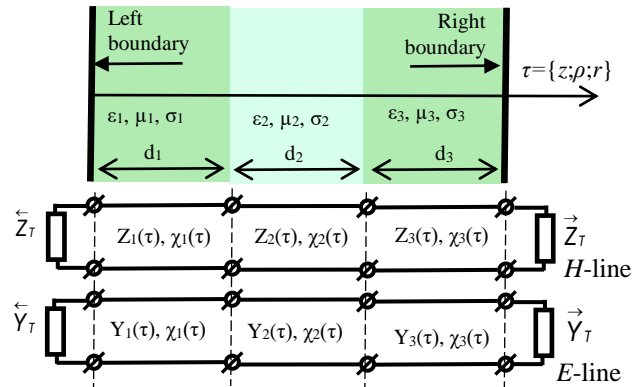


Fig. 2. The layered structure and the equivalent circuit model with magnetic (upper) and electric (lower) lines

Layer $[C_i]$ and boundary $[\Gamma_i]$ transfer matrices are used to calculate modal voltages and currents in the presence of extraneous sources (Fig.3).

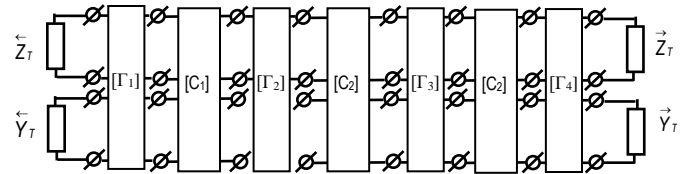


Fig.3 The layer and boundary transfer matrices for the layered structure mode

Boundary conditions at the ends of the interval are modeled by terminal loads. The directional resistance \bar{Z}_T and conductivity \bar{Y}_T as well as resistance \bar{Z}_T and conductivity \bar{Y}_T are used as inner and outer terminal loads, respectively. The expressions for terminal loads are shown in Table I and Table II. It should be noted that the value of the wave resistances Z_i and admittances Y_i as well as propagation constants χ_i in equivalent E - and H -lines depend on the radial coordinate in the cylindrical and spherical coordinate systems and remain constant in the Cartesian coordinate system (Table III).

TABLE I. THE EXPRESSIONS FOR OUTER TERMINAL LOADS

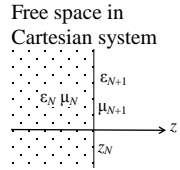
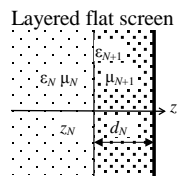
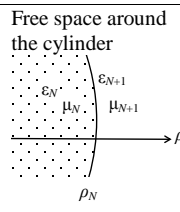
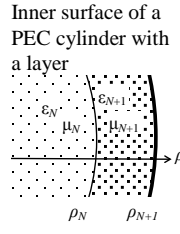
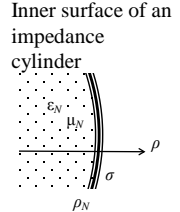
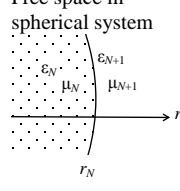
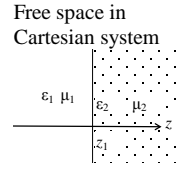
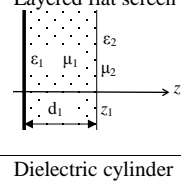
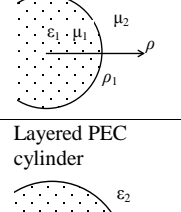
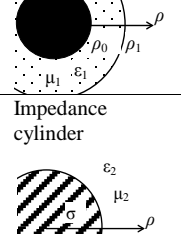
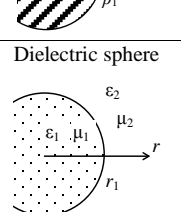
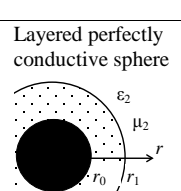
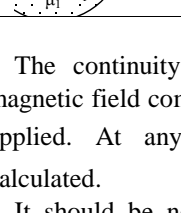
Region boundary	Outer Terminal Loads \bar{Y}_T, \bar{Z}_T
Free space in Cartesian system 	$\bar{Y}_N^+ = Y_0$ $\bar{Z}_N^+ = Z_0$
Layered flat screen 	$\bar{Y}_N^+ = -jY_0 \frac{\gamma_{N+1}}{k_{N+1}} \cot \gamma_{N+1} d_{N+1},$ $\gamma_{N+1} = \sqrt{k_{N+1}^2 - \xi^2 - \eta^2}$ $\bar{Z}_N^+ = jZ_0 \frac{\gamma_{N+1}}{k_{N+1}} \tan \gamma_{N+1} d_{N+1},$ $\gamma_{N+1} = \sqrt{k_{N+1}^2 - \xi^2 - \eta^2}$
Free space around the cylinder 	$\bar{Y}_N^+ = jY_0 \frac{k_0^2 \rho_N}{\gamma_{N+1}} \frac{H_m^{(2)'(\gamma_{N+1} \rho_N)}}{H_m^{(2)}(\gamma_{N+1} \rho_N)}, \gamma_{N+1} = \sqrt{k_0^2 - h^2}$ $\bar{Z}_N^+ = jZ_0 \frac{k_0^2 \rho_N}{\gamma_{N+1}} \frac{H_m^{(2)'(\gamma_{N+1} \rho_N)}}{H_m^{(2)}(\gamma_{N+1} \rho_N)}, \gamma_{N+1} = \sqrt{k_0^2 - h^2}$
Inner surface of a PEC cylinder with a layer 	$\bar{Y}_N^+ = jY_0 \frac{\epsilon'_{N+1} k_0^2 \rho_N}{\gamma_{N+1}} \frac{C_{1m}(\gamma_{N+1} \rho_N, \gamma_{N+1} \rho_{N+1})}{S_{2m}(\gamma_{N+1} \rho_N, \gamma_{N+1} \rho_{N+1})}$ $\bar{Z}_N^+ = jZ_0 \frac{\mu'_{N+1} k_0^2 \rho_N}{\gamma_{N+1}} \frac{S_{1m}(\gamma_{N+1} \rho_N, \gamma_{N+1} \rho_{N+1})}{C_{2m}(\gamma_{N+1} \rho_N, \gamma_{N+1} \rho_{N+1})}$
Inner surface of an impedance cylinder 	$\bar{Y}_N^- = k_0 \rho_N \sqrt{\frac{2\sigma}{\omega \mu_0}} \frac{(1-j)}{2}$ $\bar{Z}_N^- = k_0 \rho_N \sqrt{\frac{\omega \mu_0}{2\sigma}} (1+j)$
Free space in spherical system 	$\bar{Y}_N^+ = jY_0 \frac{h_m^{(2)'(k_0 r_N)}}{h_m^{(2)}(k_0 r_N)}$ $\bar{Z}_N^+ = jZ_0 \frac{h_m^{(2)'(k_0 r_N)}}{h_m^{(2)}(k_0 r_N)}$

TABLE II. THE EXPRESSIONS FOR INNER TERMINAL LOADS

Region boundary	Inner Terminal Loads \bar{Y}_T, \bar{Z}_T
Free space in Cartesian system 	$\bar{Y}_1^- = Y_0$ $\bar{Z}_1^- = Z_0$
Layered flat screen 	$\bar{Y}_1^- = -jY_0 \frac{\epsilon'_1 k_0}{\gamma_1} \cot \gamma_1 d_1, \gamma_1 = \sqrt{k_1^2 - \xi^2 - \eta^2}$ $\bar{Z}_1^- = jZ_0 \frac{\mu'_1 k_0}{\gamma_1} \tan \gamma_1 d_1, \gamma_1 = \sqrt{k_1^2 - \xi^2 - \eta^2}$
Dielectric cylinder 	$\bar{Y}_1^- = -jY_0 \frac{\epsilon'_1 k_0^2 \rho_1}{\gamma_1} \frac{J'_m(\gamma_1 \rho_1)}{J_m(\gamma_1 \rho_1)}, \gamma_1 = \sqrt{k_1^2 - h^2}$ $\bar{Z}_1^- = -jZ_0 \frac{\mu'_1 k_0^2 \rho_1}{\gamma_1} \frac{J'_m(\gamma_1 \rho_1)}{J_m(\gamma_1 \rho_1)}, \gamma_1 = \sqrt{k_1^2 - h^2}$
Layered PEC cylinder 	$\bar{Y}_1^- = jY_0 \frac{\epsilon'_1 k_0^2 \rho_1}{\gamma_1} \frac{C_{1m}(\gamma_1 \rho_1, \gamma_1 \rho_0)}{S_{2m}(\gamma_1 \rho_1, \gamma_1 \rho_0)}, \gamma_1 = \sqrt{k_1^2 - h^2}$ $\bar{Z}_1^- = jZ_0 \frac{\mu'_1 k_0^2 \rho_1}{\gamma_1} \frac{S_{1m}(\gamma_1 \rho_1, \gamma_1 \rho_0)}{C_{2m}(\gamma_1 \rho_1, \gamma_1 \rho_0)}, \gamma_1 = \sqrt{k_1^2 - h^2}$
Impedance cylinder 	$\bar{Y}_1^- = \bar{Y}_1^+ = -k_0 \rho_1 \sqrt{\frac{2\sigma}{\omega \mu_0}} \frac{(1-j)}{2}$ $\bar{Z}_1^- = \bar{Z}_1^+ = -k_0 \rho_1 \sqrt{\frac{\omega \mu_0}{2\sigma}} (1+j)$
Dielectric sphere 	$\bar{Y}_1^- = -jY_0 \sqrt{\frac{\epsilon'_1}{\mu'_1}} \frac{j'_m(k_1 r_1)}{j_m(k_1 r_1)}$ $\bar{Z}_1^- = -jZ_0 \sqrt{\frac{\mu'_1}{\epsilon'_1}} \frac{j'_m(k_1 r_1)}{j_m(k_1 r_1)}$
Layered perfectly conductive sphere 	$\bar{Y}_1^- = -jY_0 \sqrt{\epsilon'_1} \frac{s'_n(k_1 r_1, k_1 r_0)}{s_n(k_1 r_1, k_1 r_0)}$ $\bar{Z}_1^- = -j \frac{Y_0}{\sqrt{\epsilon'_1}} \frac{c'_n(k_1 r_1, k_1 r_0)}{c_n(k_1 r_1, k_1 r_0)}$

In the Table I and Table II the index N is the number of the last layer, $H_m^{(2)}, H_m^{(2)'}, J_m, J'_m, h_m^{(2)}, h_m^{(2)'}, j_m$ and j'_m are cylindrical and spherical Hankel and Bessel functions and its derivative, respectively. The functions $C_{1m}, S_{2m}, S_{1m}, C_{2m}, s_n, s'_n, c_n$ and c'_n are the combination of the cylindrical and spherical functions of the 1-st and 2-nd kind, respectively [8]. The plus sign indicates that we determine the input resistance or admittance in the equivalent circuit to the right of the boundary. The minus sign shows that we define these values to the left of the boundary. The value $Z_0 = Y_0^{-1} = 120\pi$ Ohm.

The continuity condition of the tangential electric and magnetic field components at the boundaries between layers is applied. At any boundary the transfer matrix $[\Gamma_N]$ is calculated.

It should be noted that for covered perfectly conductive cylinder the expressions for the inner loads \bar{Y}_1^- and \bar{Z}_1^- from the Table II of the equivalent circuit are converted to the form

$$\bar{Y}_1^- \cong -jY_0 \frac{\epsilon'_1}{\gamma_1} k_0^2 \rho_1 \cot \gamma_1 \Delta \rho, \quad \bar{Z}_1^- \cong jZ_0 \frac{\mu'_1}{\gamma_1} k_0^2 \rho_1 \tan \gamma_1 \Delta \rho,$$

if $\rho_1 - \rho_0 = \Delta\rho$, $\Delta\rho \ll \rho_0$, where ρ_0 is the outer radius of the perfectly conductive cylinder, $\Delta\rho$ is the layer thickness. They are the same as for a flat perfectly conductive screen with a slab in Cartesian system.

TABLE III. EQUIVALENT LINE PARAMETERS IN DIFFERENT COORDINATE SYSTEMS

Coordinate system	Equivalent line Characteristic of the <i>i</i> -th Layer	
	Parameter	Expression
Cartesian	Wave admittance of <i>E</i> -line	$Y_i = Y_0 \sqrt{\epsilon'_i / \mu'_i}$
	Wave impedance of <i>H</i> -line	$Z_i = Z_0 \sqrt{\mu'_i / \epsilon'_i}$
	Propagation constant	$\chi_i = k_i$
Cylindrical	Wave admittance of <i>E</i> -line	$Y_i = Y_0 \frac{k_0^2 \epsilon'_i \rho}{\gamma_i^2} \sqrt{\gamma_i^2 - \left(\frac{m}{\rho}\right)^2}$
	Wave impedance of <i>H</i> -line	$Z_i = Z_0 \frac{k_0^2 \mu'_i \rho}{\gamma_i^2} \sqrt{\gamma_i^2 - \left(\frac{m}{\rho}\right)^2}$
	Propagation constant	$\chi_i = \sqrt{\gamma_i^2 - \left(\frac{m}{\rho}\right)^2}, \gamma_i = \sqrt{k_i^2 - h^2}$
Spherical	Wave admittance of <i>E</i> -line	$Y_i = Y_0 k_0 \epsilon'_i / \chi_i$
	Wave impedance of <i>H</i> -line	$Z_i = Z_0 k_0 \mu'_i / \chi_i$
	Propagation constant	$\chi_i = \sqrt{k_i^2 - \left(\frac{m(m+1)}{r}\right)^2}$

In the Table III index *m* is the integer constant from Helmholtz equation of axial components of the electric and magnetic fields in the cylindrical coordinates and of radial components in the spherical coordinates system. In the *i*-th layer the wave number is k_i , the permittivity is ϵ'_i and the magnetic permeability is μ'_i , respectively.

Wave propagation in each layer is described with 8-port network and the transmitting matrix $[C_i]$. As there is no energy exchange between electric and magnetic waves in the homogeneous medium inside every layer equivalent *E* and *H*-lines are unconnected. So, transmitting matrixes become simplified

$$[C_i] = \begin{bmatrix} [C_{iE}] & [0] \\ [0] & [C_{iH}] \end{bmatrix},$$

where $[0]$ is a null matrix of order 2. Two ports network with the transfer matrix $[C_{iE}]$ is associated with the equivalent electric line and another two ports network with the transfer matrix $[C_{iH}]$ is associated with the equivalent magnetic line.

Unlike the flat and spherical structures, the boundary conditions at the layers' boundaries in the cylindrical structure cause energy exchange between *E* and *H* waves that occurs as in coupling lines. Taking into account the coupling of *E* and *H*-lines the 4-port boundary network with transmitting matrix $[\Gamma_i]$ of order 4 is added for the cylindrical structures.

$$[\Gamma_i] = \begin{bmatrix} 1 & 0 & 0 & 0 \\ 0 & 1 & 0 & -N_i \\ N_i & 0 & 1 & 0 \\ 0 & 0 & 0 & 1 \end{bmatrix},$$

where $N_i = \frac{mh}{k_0} \left(\frac{1}{\gamma_i^2} - \frac{1}{\gamma_{i+1}^2} \right)$, $\gamma_i = \sqrt{k_i^2 - h^2}$.

As there is no energy exchange at boundaries in flat and spherical structures, the matrix $[\Gamma_i]$ is a unit matrix.

Thus, the expressions for Green's functions are as follows.

For Cartesian coordinates

$$\begin{aligned} \bar{\bar{\Gamma}}_{ij}(x, y, z; x', y', z') &= \\ &= j\omega\mu_0 \int_{-\infty}^{\infty} \int_{-\infty}^{\infty} F \{g(z; z'), f(z; z')\} G_t(x, y; x', y') d\xi d\eta, \end{aligned} \tag{3}$$

where for unlimited space along *x* and *y* coordinates

$$G_t(x, y; x', y') = \frac{1}{4\pi} e^{-i\xi(x-x')} e^{-i\eta(y-y')}.$$

In (3) characteristic functions $g(z; z')$ and $f(z; z')$ are the solution the differential equations with proper boundary conditions as follows

$$\begin{aligned} \frac{d^2 f(z, z')}{dz^2} + \gamma^2 f(z, z') &= -\delta(z - z'), \\ \frac{d^2 g(z, z')}{dz^2} + \gamma^2 g(z, z') &= -\delta(z - z'). \end{aligned}$$

If the boundary is the perfect conductor, we have at this section $f(z, z') = \frac{dg(z, z')}{dz} = 0$.

For the cylindrical coordinate system Green's functions are define as follows

$$\begin{aligned} \bar{\bar{\Gamma}}_{ij}(\rho, \varphi, z; \rho', \varphi', z') &= \\ &= -j \frac{\omega\mu_0}{2\pi} \sum_{m=-\infty}^{\infty} \int_{-\infty}^{\infty} F \{g_m(\rho; \rho'), f_m(\rho; \rho')\} G_t(m, h, \varphi, z; \varphi', z') dh, \end{aligned}$$

where

$$G_t(m, h, \varphi, z; \varphi', z') = \frac{1}{2\pi} e^{-jm(\varphi-\varphi')} e^{-jh(z-z')}.$$

The characteristic functions $g_m(\rho; \rho)$ and $f_m(\rho; \rho)$ are the solution the differential equations

$$\begin{aligned} \frac{1}{\rho} \frac{d}{d\rho} \left(\rho \frac{dg_m(\rho; \rho')}{d\rho} \right) + \left(k^2 - h^2 - \frac{m^2}{\rho^2} \right) g_m(\rho; \rho') &= -\delta(\rho - \rho'), \\ \frac{1}{\rho} \frac{d}{d\rho} \left(\rho \frac{df_m(\rho; \rho')}{d\rho} \right) + \left(k^2 - h^2 - \frac{m^2}{\rho^2} \right) f_m(\rho; \rho') &= -\delta(\rho - \rho'). \end{aligned}$$

If the spherical structures are under consideration the Green's functions are defined as

$$\begin{aligned} \bar{\bar{\Gamma}}_{ij}(\theta, \varphi, r; \theta', \varphi', r') &= \\ &= j\omega\mu_0 \sum_{n=0}^{\infty} \sum_{m=-n}^n F \{g_n(r; r'), f_n(r; r')\} G_t(m, n, \theta, \varphi; \theta', \varphi'), \end{aligned}$$

where

$$G_t(m, n, \theta, \varphi; \theta', \varphi') = \frac{1}{4\pi} \Phi \left\{ P_n^m(\cos \theta) e^{-jm\varphi}, P_n^m(\cos \theta') e^{jm\varphi'} \right\}.$$

The spherical harmonics are calculated using the associated Legendre polynomials $P_n^m(\cos \theta)$.

The characteristic functions are the solution of the inhomogeneous equations

$$\frac{d^2 g_n(r, r')}{dr^2} + k^2 g_n(r, r') = -\delta(r - r'),$$

$$\frac{d^2 f_n(r, r')}{dr^2} + k^2 f_n(r, r') = -\delta(r - r').$$

Thus Green's functions for three main coordinate systems such as Cartesian, cylindrical and spherical are given. A wide class of electromagnetic excitation, radiation, and diffraction problems can be solved using the appropriate distribution of extraneous currents. The using of analytical approaches allows one significantly speed up the calculation in electromagnetics.

III. WAVE REFLECTION ANALYSIS AS A RADIATION PROBLEM SOLVING

We applied the Green's function method for spherical and cylindrical Luneburg lens investigation [9]. It was successfully used for spherical and geodesic antenna radomes analysis [10]. Application of Green's functions for diffraction problems solving is described in this part.

The synthesis of surfaces with the required reflecting properties is an actual problem of electrodynamics. Of particular interest are the problems of non-reflecting and selectively reflecting covers synthesis [11], [12]. Layered structures are widely used for non-reflecting coating design.

The flat multilayered structure under consideration is shown in Fig.4. Thickness, dielectric permittivity and the magnetic permeability as conductivity of any layer have arbitrary value. We use the parallel and perpendicular electrical field components relative to the incidence plane. The reflected waves generated by a layered structure are calculated as radiation of the equivalent electric and magnetic surface currents located at the illuminated side of the covered conducting screen. Equivalent electric and magnetic surface currents for the incident wave are specified as

$$\mathbf{J} = \mathbf{n} \times \mathbf{H}, \quad \mathbf{M} = \mathbf{E} \times \mathbf{n}, \quad (4)$$

where \mathbf{H} and \mathbf{E} are magnetic and electric incident wave components at the illuminated surface, respectively, \mathbf{n} is a normal to this surface.

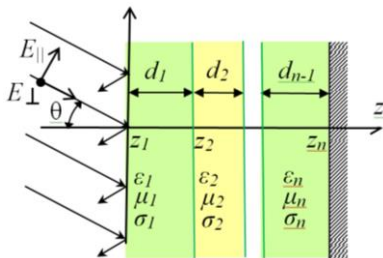


Fig. 4. An incident wave with perpendicular and parallel electrical field vector near the multilayered structure

We define equivalent surface current density for the incident angle θ with respect to the surface normal as following. For the parallel polarization equivalent surface currents are specified as

$$M_x = -E_0 \cos \theta e^{-jk_0 x \sin \theta},$$

$$J_y = E_0 Y_0 e^{-jk_0 x \sin \theta},$$

for the perpendicular polarization we have

$$M_y = E_0 e^{-jk_0 x \sin \theta}$$

$$J_x = E_0 Y_0 \cos \theta e^{-jk_0 x \sin \theta}$$

where E_0 is an amplitude of the incident wave, k_0 is the free-space wave number, $Y_0 = (120\pi)^{-1} \text{ Ohm}^{-1}$ is the free-space wave admittance.

After substituting (4) into (2) the total electrical field components are represented at the illuminated surface at the plane $z = z_1$ by rather simple expressions

$$E_x^t = E_0 \frac{2Y_0}{\bar{Y}_1^- + \bar{Y}_1^-} e^{-jk_0 x \sin \theta}, \quad (5)$$

$$E_y^t = -E_0 \frac{2Y_0 \cos \theta}{\bar{Z}_1^- + \bar{Z}_1^-} e^{-jk_0 x \sin \theta}. \quad (6)$$

The input directional admittances and impedances of the equivalent circuit are shown in the Table I and Table II. The reference plane is located at $z = z_1$. There are several layers to the right from the reference plane so input directional admittance and impedance to the right from the reference plane are calculated by recurrent formulas

$$\bar{Y}_{i-1} = Y_i \frac{\bar{Y}_i \text{ctg } \gamma_i d_i + jY_i}{Y_i \text{ctg } \gamma_i d_i + j\bar{Y}_i},$$

$$\bar{Z}_{i-1} = Z_i \frac{\bar{Z}_i \text{ctg } \gamma_i d_i + jZ_i}{Z_i \text{ctg } \gamma_i d_i + j\bar{Z}_i}.$$

If there is a free space at $z > z_1$ and no reflecting waves, the incident wave components are defined as

$$E_x^{inc} = E_0 \cos \theta e^{-jk_0 x \sin \theta},$$

$$E_y^{inc} = -E_0 e^{-jk_0 x \sin \theta}, \quad (8)$$

Subtracting (8) from (9) and (10) we evaluate reflection coefficients by the following two formulas

$$R_x = \frac{Y_0 / \cos \theta - \bar{Y}_1^-}{\bar{Y}_1^- + \bar{Y}_1^-} e^{-jk_0 x \sin \theta}, \quad (9)$$

$$R_y = \frac{Z_0 \cos \theta - \bar{Z}_1^-}{\bar{Z}_1^- + \bar{Z}_1^-} e^{-jk_0 x \sin \theta}. \quad (10)$$

The terminal conductivity and impedance at the screen plane $z = z_N$ are defined as $\bar{Y}_N = Y_0 \sqrt{-j\sigma/Y_0 k_0}$ and $\bar{Z}_{NE} = Z_0 \sqrt{j k_0 / \sigma Z_0}$ for real conductors, where σ is metal conductivity. For the perfect conductor $\bar{Y}_{NE} \rightarrow -j\infty$ and $\bar{Z}_{NE} = 0$.

The proposed approach is not limited by the number of layers under consideration. The electrodynamic properties of ϵ_i , μ_i , σ_i of each layer material are arbitrary. Magnetic losses may be taken into account as well. The approach remains correct for materials with negative refractive index. For example, consider a two-layer structure. The task is to minimize the reflection coefficient at a frequency of 10 GHz.

In [13] the absorber based on carbon nanofibers (CNF 3 wt%) was analyzed. It was noted that the considered cover of 6.5 mm thickness does not allow one to obtain the reflection of less than minus 6 dB. However, if we place a magneto-dielectric layer on the top of this slab the reflection coefficient is significantly reduced. We have optimized the two-layer structure. We have shown that it is possible to obtain a reflection coefficient of less than minus 35 dB for large range of incident angles with the same thickness of the composite cover limited by 6.5 mm (Fig.5).

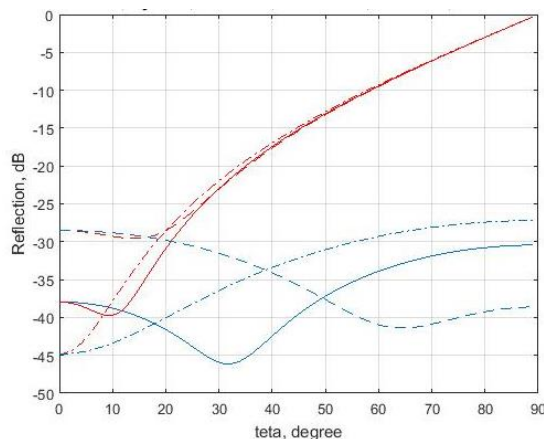


Fig. 5. Reflection of the incident wave with perpendicular and parallel polarization from the two-layer structure with PEC backing ($\epsilon_1=1.7-j2.0$, $\epsilon_2=13.1-j6.5$, $\mu_1=1.5-j2.0$, $\mu_2=1.0-j0.0$): $d_1=3$ mm, $d_2=3.5$ mm (dash line), $d_1=3.5$ mm, $d_2=3.0$ mm (solid line), $d_1=4.0$ mm, $d_2=2.5$ mm (dash-dot line). Parallel polarization is marked in red, perpendicular polarization is marked in blue.

The frequency properties of the two-layer absorbing coating with a magneto-dielectric slab for different angles of wave incidence are illustrated in Fig.6. It is noted that the reflection of less than minus 20 dB is observed from 5.5 GHz. Parallel polarization is marked in red, perpendicular polarization is marked in blue. For the normal angle of wave incidence, the graphs of the reflection coefficients coincide (is marked in black).

We showed the solution of a simple problem with simple formulas. Usually derivation of expressions for calculations is rather complicated. This hard work is more than compensated by fast calculations using compact formulas.

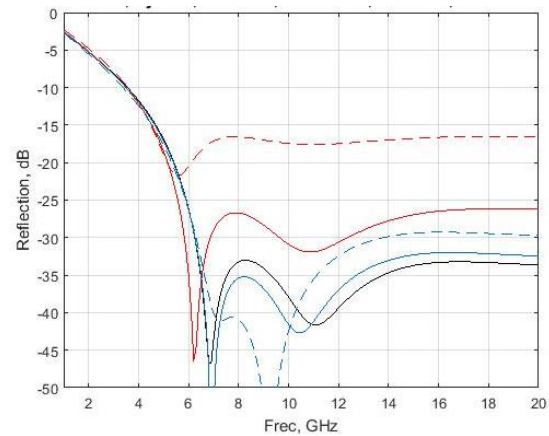


Fig. 6. Reflection coefficient from the two-layer composite with PEC backing ($\epsilon_1=1.7-j2.0$, $\epsilon_2=13.1-j6.5$, $\mu_1=1.5-j2.0$, $\mu_2=1.0-j0.0$, $d_1=3$ mm, $d_2=3.5$ mm: $\theta=0^\circ$ (black line), $\theta=20^\circ$ (solid line), $\theta=40^\circ$ (dash line). Parallel polarization is marked in red, perpendicular polarization is marked in blue.

ACKNOWLEDGMENT

The research was supported by the grant of the Ministry of education and science of the Russian Federation (project № 8.2538.2017/4.6).

REFERENCES

- [1] L. Sevgi, *Electromagnetic Modeling and Simulation*, Wiley-IEEE Press, 2014.
- [2] J. Volakis, *Antenna Engineering Handbook*, Fourth Edition, McGraw-Hill Education, 2007.
- [3] C.A. Balanis, *Antenna Theory: Analysis and Design*, John Wiley & Sons, Inc., 2016.
- [4] D. B. Davidson, *Computational Electromagnetics for RF and Microwave Engineering*, Second Edition, Cambridge University Press, 2010
- [5] B. Fuchs, L. Le Coq, O. Lafond, and S.Rondineau, "Design Optimization of Multishell Luneburg Lenses," *IEEE Trans. Antennas and Propag.*, vol. 55, no 2. pp. 283-289, 2007.
- [6] D. Micheli; R. Pastore; M. Marchetti; G. Gradoni; F. Moglie, and V. M. Primiani, "Modeling and measuring of microwave absorbing and shielding nanostructured materials", *Proc. International Symposium on Electromagnetic Compatibility - EMC EUROPE*, Rome, Italy, 2012.
- [7] L. B. Felsen, N. Marcuvitz, *Radiation and Scattering of Waves*. Englewood Cliffs: Prentice Hall, 1973.
- [8] S. Dailis and S. Shabunin "Microstrip antennas on metallic cylinder covered with radially inhomogeneous magnetodielectric" in *Proc. of 9th Int. Wroclaw Symp. on Electron. Compatib.*, Part 1, Wroclaw, Poland, pp. 271-277, 1988.
- [9] S. Knyazev, A. Korotkov, B. Panchenko, S. Shabunin, "Investigation of spherical and cylindrical Luneburg lens antennas by the Green's function method", *IOP Conference Series: Materials Science and Engineering*, 2016, 120 (1), 012011.
- [10] A.Karpov, S. Knyazev, L. Lesnaya, S. Shabunin, "Sandwich Spherical and Geodesic Antenna Radomes Analysis", *Proc. of the 10th European Conference on Antennas and Propagation (EuCAP 2016)*, Davos, Switzerland, 2016, pp. 1-5.
- [11] E. F. Knoff, "RCSR Guidelines Handbook", Engineering Experiment Station, Georgia Institute of Technology, 1976.
- [12] W. Emerson, "Electromagnetic wave absorbers and anechoic chambers through the years", *IEEE Trans. on Antennas and Propag.*, vol. 21, no 4, pp. 484-490, 1973.
- [13] D. Micheli; R. Pastore; M. Marchetti; G. Gradoni; F. Moglie, and V. M. Primiani, "Modeling and measuring of microwave absorbing and shielding nanostructured materials", in *Proc. International Symposium on Electromagnetic Compatibility - EMC EUROPE*, Rome, Italy, 2012.